

Catalytic performance of bimetallic Ni-Pt nanoparticles supported on activated carbon, gamma-alumina, zirconia, and ceria for hydrogen production in sulfur-iodine thermochemical cycle

Amit Singhanian^a, Venkatesan V. Krishnan^{a, #}, Ashok N. Bhaskarwar^{a*}, Bharat Bhargava^b,
Damaraju Parvatalu^b, Satinath Banerjee^b

^aDepartment of Chemical Engineering, Indian Institute of Technology Delhi, Hauz Khas, New Delhi 110016, India

^bONGC Energy Centre, 2nd Floor, Core-2, Scope Minar, New Delhi 110092, India

*Corresponding author. Tel.: +91-01126591028; Email: ashoknbhaskarwar@yahoo.co.in (Ashok N. Bhaskarwar)

Current Address: Teesside University, School of Science and Engineering, Middlesbrough, TS1 3BA, UK

ABSTRACT

Bimetallic Ni-Pt nanoparticles supported on four different supports (activated carbon (AC))¹, γ -alumina, zirconia, and ceria) were prepared by modified impregnation-reduction technique for decomposition of hydrogen iodide to hydrogen and iodine, in the thermochemical water- splitting

¹Abbreviations

AC	Activated carbon	TOS	Time on stream
MoC	Material of construction	WHSV	Weight hourly space velocity, h ⁻¹
SI	Sulfur-iodine		

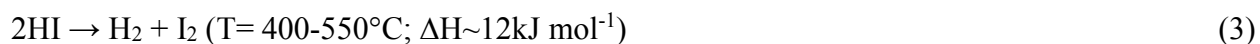
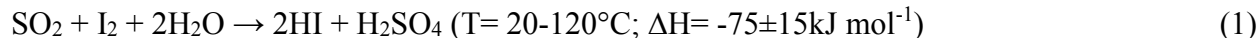
sulfur-iodine (SI) cycle. The catalysts were characterized by powder X-ray diffraction (XRD), transmission electron microscopy (TEM), and Brunauer–Emmett–Teller (BET) method to find their structure, morphology, and surface area, respectively. High metal dispersions (Ni-Pt) were obtained with particle sizes of the order of 10 nm or lesser, in the high-surface-area supports. The hydrogen iodide-decomposition results showed the following catalytic activity order of Ni-Pt nanoparticles on different supports: Ni(2.5%)-Pt(2.5%)/AC > Ni(2.5%)-Pt(2.5%)/ γ -alumina > Ni(2.5%)-Pt(2.5%)/Zirconia > Ni(2.5%)-Pt(2.5%)/Ceria. Bimetallic Ni(2.5%)-Pt(2.5%)/AC also showed excellent stability for 100 h in the hydrogen iodide-decomposition reaction, and with a higher performance relative to the corresponding Pt supported catalyst under the same operating conditions.

Keywords: SI thermochemical cycle, Nickel, Platinum, Hydrogen iodide-decomposition, Hydrogen production

1. Introduction

Hydrogen is probably an ultimately vital energy carrier for the future, where fossil fuels are expected to be scarce [1–3]. While there are exciting possibilities in the manufacture of hydrogen from renewable sources, primarily water and biomass, there are also non-electrochemical pathways to achieve hydrogen production, notably by the use of cyclic pathways that can tap into very high quality heat, available in nuclear power plants. The sulfur–iodine (SI) thermochemical cycle is one such method for hydrogen production [4]. Over the past few decades, many researchers have studied the potential of the SI process for large-scale hydrogen production [5–

11], although the process still remains considerably un-optimized. The SI cycle consists of the following reactions [12].

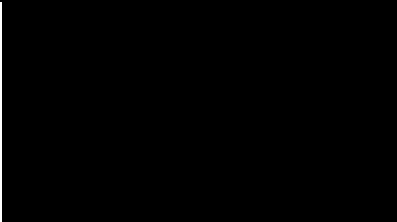
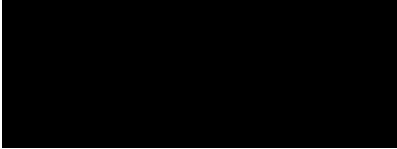


The net advantage of this cycle is the decomposition of water into hydrogen and oxygen without emission of any greenhouse gas. The iodine and sulfur dioxide produced in the hydrogen iodide-decomposition and sulfuric-acid decomposition reactions, respectively, are separated and recycled to the Bunsen reactor. Since two of the three reactions are considerably endothermic and require very high temperature, this type of thermochemical splitting of water is achievable only when waste heat is available at temperatures of about 1000°C, i.e. in nuclear power plants. Thus, nuclear power plants may be used effectively to produce large quantity of hydrogen which can be bottled, stored, and supplied for a variety of applications including transportation and clean backup power for telecom applications.

Hydrogen iodide-decomposition, in addition to being highly endothermic, is strongly equilibrium limited under desirable reaction conditions of about 400°C to 600°C. As per the reaction stoichiometry, the equilibrium yields are independent of pressure. A highly active and stable catalyst is targeted for the production of hydrogen from hydrogen iodide in the SI cycle. The principal aim of catalyst development is such that the reaction achieves near-equilibrium conversions at commercial space velocities and at temperatures, where corrosion by hydrogen iodide and iodine is minimal, and where expensive materials of construction (MoC) are not necessary. A reaction temperature of no higher than 550°C is therefore optimal, so that the appropriate MoCs can be used. A review of MoCs and ‘usable’ temperatures for hydrogen iodide

reaction is shown in the following table 1 which lists the MoC candidates with their stand-up temperatures.

Table 1. MoC candidates with their stand-up temperatures for hydrogen iodide reaction.

Materials	Tested temperature	Stability	Remarks on General Costing/ usage
SiC and Borosilicate glass [13]	200°C	Stable up to 200°C	
Zr [14]	310°C	Not stable at 310°C	
Ta and Ta-Nb based alloys [14]	310°C	Stable up to 310°C	Very high cost as compared to Hastelloy and Alloy 617 [16] – Not useful
C-276 [14]	310°C	Not stable up to 310°C	
Mullite [14]	310°C	Not stable up to 310°C	
Hastelloy [15]	450°C	Stable up to 450°C	Less as compared to Alloy 617 and Ta-Nb based alloys [16]
Alloy 617 [16]	850°C	Stable up to 850°C	High as compared to Hastelloy [16]

With the above information, a target design temperature for operating the reactor appears to be around 450°C, and possibly up to 550°C. At very low temperatures where MoCs like SiC and borosilicate glass are applicable, the kinetics are very slow, and at 850°C, where kinetics are very

rapid, the MoCs are very expensive. Therefore, the operating temperatures of the reaction are limited to the range of 450°C-550°C, where Hastelloy can be used as the MoC.

Different catalysts, including noble metal catalysts (Au and Pt [17–19], Ni, Pd, and bimetallic catalysts [20–25]) have been reported in literature along with a variety of support materials (activated carbon (AC), ceria, γ -alumina, carbon nanotubes, graphite, carbon molecular sieve [26–29]) for catalytic hydrogen iodide-decomposition. A very good review was given by O’Keeffe et al. [6] on the studies of catalysis research in SI process in which Pt supported catalysts showed good catalytic activity. Noble metal based catalysts (supported Pt-catalysts) have been extensively studied for hydrogen iodide-decomposition reaction as they show very good catalytic activity for the reaction [26-28]. Some results have indicated that performances of Pt supported catalysts were indeed influenced by the support [26]. Among the different supported Pt catalysts, Pt/AC was found to give excellent catalytic activity for hydrogen iodide-decomposition reaction. Favuzza et al. [30] also reported the high stability of AC for 140 h during hydrogen iodide-decomposition. Wang et al. [31] reported the overview of catalyst development at Institute of Nuclear and New Energy Technology, Tsinghua University, (INET), and also concluded that the future choice of catalysts for the hydrogen iodide-decomposition could either be “inexpensive catalyst (with a large quantity of AC) with large reactor” or “expensive catalyst (small quantity of supported Pt) with small reactor”. Bell [32] suggested that with approaches based on nanoscience and nanotechnology, the catalyst activity can be further enhanced by modifying the support. He explained that the catalyst activity depended on its size, shape, and structure along with the use of nanoporous supports. By controlling the size and shape of nanoporous supports, the catalyst performance can be increased.

Bimetallic catalysts have been studied for various catalytic reactions such as catalytic reforming, oxidation-reduction organic reactions, hydrogen generation, and fuel-cell electrocatalysis [33–41]. Various methods are available for the production of supported bimetallic catalysts such as co-precipitation [42], sol-gel [43], hydrothermal [44], impregnation–calcination [21], and electroless deposition [45].

The supported Pt-catalysts were found to be not stable at high temperatures during hydrogen iodide-decomposition and showed agglomeration of Pt nanoparticles (Pt/AC = 5.1 nm and used Pt/AC = 16 - 22 nm) [26-28]. Further, the addition of second metal atoms along with Pt metal into supported Pt-catalysts resulted into high sintering resistance of Pt nanoparticles during hydrogen iodide-decomposition [23-25]. Ni is a very good option along with Pt metal, as it is not only cheap but also active for hydrogen iodide-decomposition reaction [20,21]. It has been confirmed that bimetallic catalysts have better activity and stability than monometallic catalysts in many other catalytic reactions also [46-48]. Wang et al. [23] described that the stability of Pt based bimetallic catalysts was due to alloying of Pt and other transition metals like Pd, Rh, and Ni (Pt/M = 2, where M = Pd, Rh or Ni) at 500°C. Wang et al. [24] explained that the stability of Pt-Ir bimetallic catalysts might be due to alloying of Pt and Ir (Pt/Ir = 0.5, 0.9, 2) at high temperatures (500°C).

In the present paper, we have reported the synthesis of a well-known bimetallic Ni-Pt catalyst but on the surface of different supports (AC, γ -alumina, zirconia, and ceria) and their catalytic activity towards hydrogen production from hydrogen iodide. Here, we have reported a modified impregnation-reduction method for loading of bimetallic Ni-Pt on different supports with the intent of generating stable nanoparticles with a high catalytic activity. This paper has also reported the results of the catalyst characterization using powder X-ray diffraction (XRD),

transmission electron microscopy (TEM), and Brunauer–Emmett–Teller (BET) technique, and correlated the catalyst performance as a function of various supports used, in a bid to isolate an effective support which is thermally and chemically stable under the highly corrosive environment of the decomposition reaction.

2. Experimental

2.1. Catalyst preparation

AC, γ -alumina, zirconia, and ceria were each used as a support. Nickel nitrate hexahydrate and hexachloroplatinic acid hexahydrate were used as Ni and Pt precursors. Sodium borohydride, sodium hydroxide, and hydrazine hydrate were used as nucleating, precipitating, and reducing agents in this method. The Ni-Pt supported catalysts were prepared by a modified impregnation-reduction method [49,50]. No protecting agent was used in this preparation method. Figure 1 shows the schematic diagram of preparation procedure of Ni-Pt catalyst loaded on different supports. Appropriate amounts of nickel nitrate hexahydrate and hexachloroplatinic acid hexahydrate were added to 150 ml of deionized water containing support. Few drops of 0.0001M sodium borohydride were added for nucleation of bimetallic Ni-Pt particles. After the addition of sodium borohydride, a few drops of 1M sodium hydroxide and 1ml of hydrazine hydrate were added to the above solution. Then, the solution was vigorously stirred at 70°C for 4 h. The suspended solid was subjected to washing 4-5 times with deionized water and then filtered off. The product catalyst was dried at 80°C in an oven for 6 h. The loading amounts of both Ni and Pt

were 2.5 %w/w. Similarly, monometallic Pt catalysts on different supports were also prepared by the above-mentioned impregnation-reduction method.

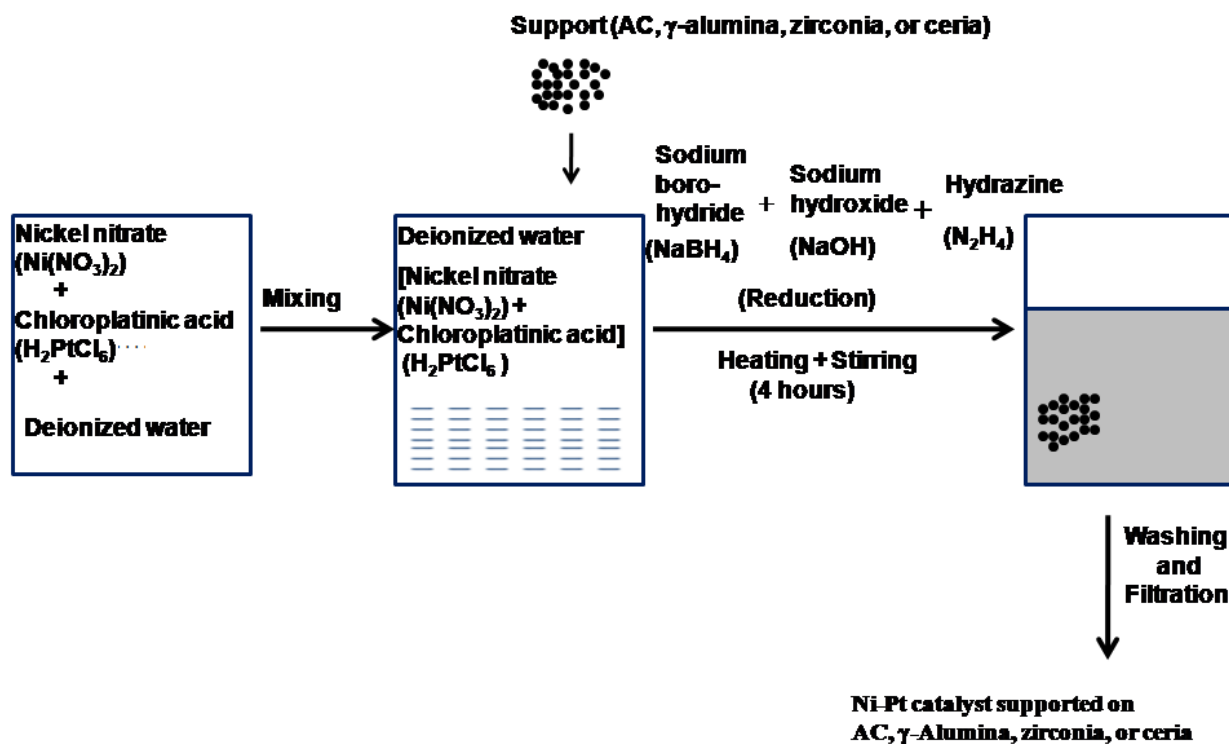


Figure 1. Schematic diagram of preparation procedure of Ni-Pt catalyst loaded on different supports.

2.2. Catalyst characterization

The specific surface area of the all the catalysts were estimated by BET technique using N_2 as adsorbate (Micrometrics, ASAP 2010). The powder XRD data of Ni-Pt supported catalysts were collected on a Rigaku X-ray diffractometer (DMAX IIIVC) which was equipped with a Ni-filtered

Cu-K α radiation ($\lambda=1.542\text{\AA}$) and a graphite crystal monochromator. The powder XRD data were collected with a step size of 0.05° and a scan rate of $2^\circ/\text{min}$. TEM micrographs were obtained on Tecnai G²-20 Twin (FEI) transmission electron microscope, operated at 200 kV. The samples were dispersed in ethanol and after 30 minutes of ultrasonication, these were deposited and dried on carbon-coated Cu grids.

2.3. Catalytic activity test

The catalytic hydrogen iodide decomposition reaction was performed in a quartz tube [16mm I.D.]. 1 g of prepared catalyst was properly homogenized with sufficient quantity of quartz particles and allowed to feed into the quartz reactor to check the performance of the catalyst. The hydrogen iodide decomposition reaction was tested at temperatures ranging from 400°C to 550°C . The hydrogen iodide (HI-55 wt%) was allowed to flow at a weight hourly space velocity (WHSV) of 12.9 h^{-1} . Nitrogen was used as a carrier gas maintained at 40 ml/min. The undecomposed hydrogen iodide, water, and product iodine were trapped using a condenser and scrubbers as shown in figure 2. The mixture of hydrogen and nitrogen gases was passed into the gas chromatograph. Hydrogen was analyzed with the help of gas chromatograph (Nucon-5765) which was equipped with a thermal conductivity detector (TCD), and in this chromatograph Molecular Sieve 5A column was used. The gas chromatograph was properly calibrated with the help of pure hydrogen gas before hydrogen iodide reaction to identify the decomposed hydrogen. Each run was conducted for 90 min. to obtain steady-state HI conversion. Figure 2 shows the schematic diagram of the experimental facility for testing of catalytic activity of prepared catalysts.

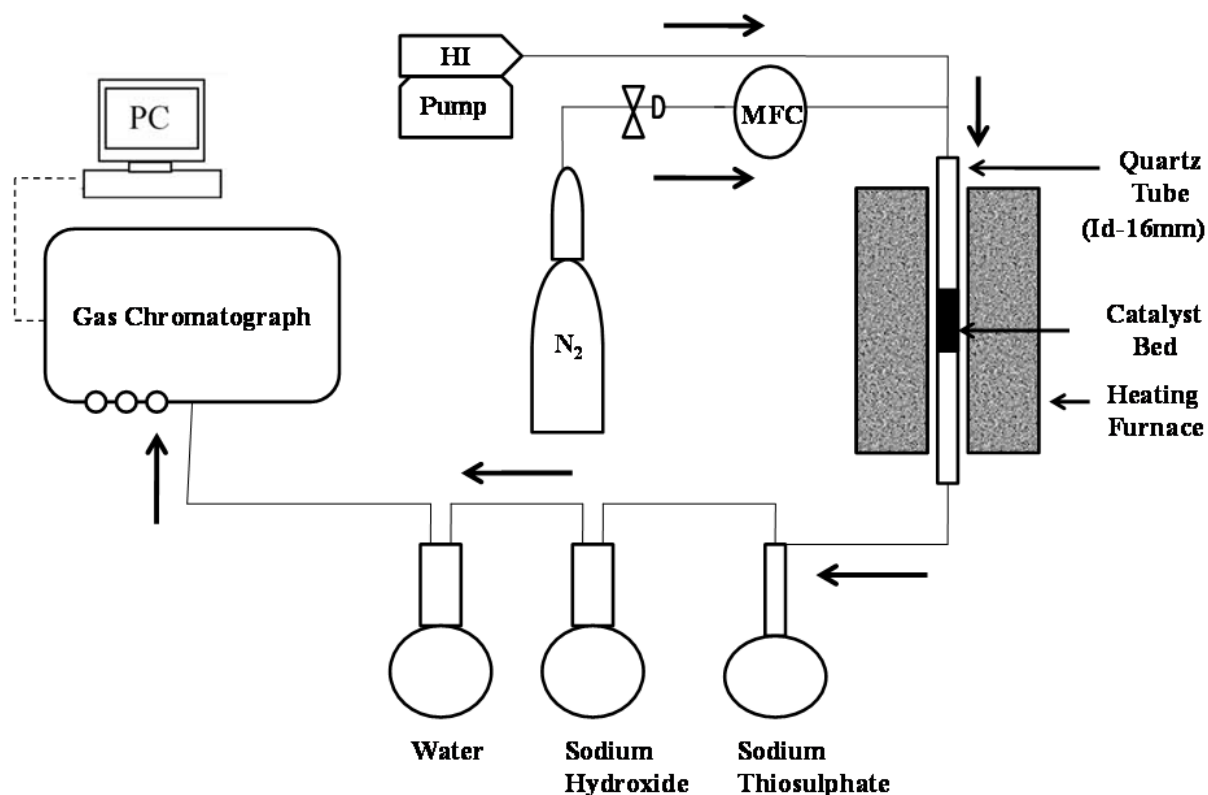


Figure 2. Schematic diagram of experimental facility for testing of catalytic activity.

3. Results and discussion

3.1. Catalyst characterization

Table 2 shows the specific surface area of all the catalysts measured by BET instrument. The specific surface area of Ni(2.5%)-Pt(2.5%)/AC catalyst is very high as compared to those of other prepared catalysts. The Ni(2.5%)-Pt(2.5%)/AC showed a specific surface area of $901.1 \text{ m}^2\text{g}^{-1}$, whereas Ni(2.5%)-Pt(2.5%)/ γ -alumina, Ni(2.5%)-Pt(2.5%)/Zirconia, and Ni(2.5%)-

Pt(2.5%)/Ceria showed a specific surface area of 223.8 m²g⁻¹, 10.5 m²g⁻¹, and 4.7 m²g⁻¹, respectively. Ni(2.5%)-Pt(2.5%)/Ceria thus showed the lowest specific surface area. The deposition of Ni-Pt on the surface of AC reduced the specific surface area from 924.2 m²g⁻¹ to 901.1 m²g⁻¹, respectively. This may be due to the blocking of some of the pores of support AC by Ni-Pt catalyst.

Table 2. BET sample characterization.

Sample code	Specific Surface area (m ² g ⁻¹)
AC	924.2
γ -alumina	245.0
Zirconia	18.6
Ceria	13.0
Ni(2.5%)-Pt(2.5%)/AC	901.1
Ni(2.5%)-Pt(2.5%)/ γ -alumina	223.8
Ni(2.5%)-Pt(2.5%)/Zirconia	10.5
Ni(2.5%)-Pt(2.5%)/Ceria	4.7

Figure 3 shows the characteristic powder XRD patterns of prepared samples. AC and γ -alumina have an amorphous structure. The XRD patterns showed highly crystalline nature of zirconia and ceria supports which is evident from the sharp peaks (figure 3). In XRD patterns of all the bimetallic catalysts, no sharp peaks corresponding to Ni or Pt crystals were found, which

shows that the metal particles are highly dispersed on the supports. Also, it is to be noted that the XRD technique is not sensitive if the amount of the catalyst phase is too low (less than 5%) [49].

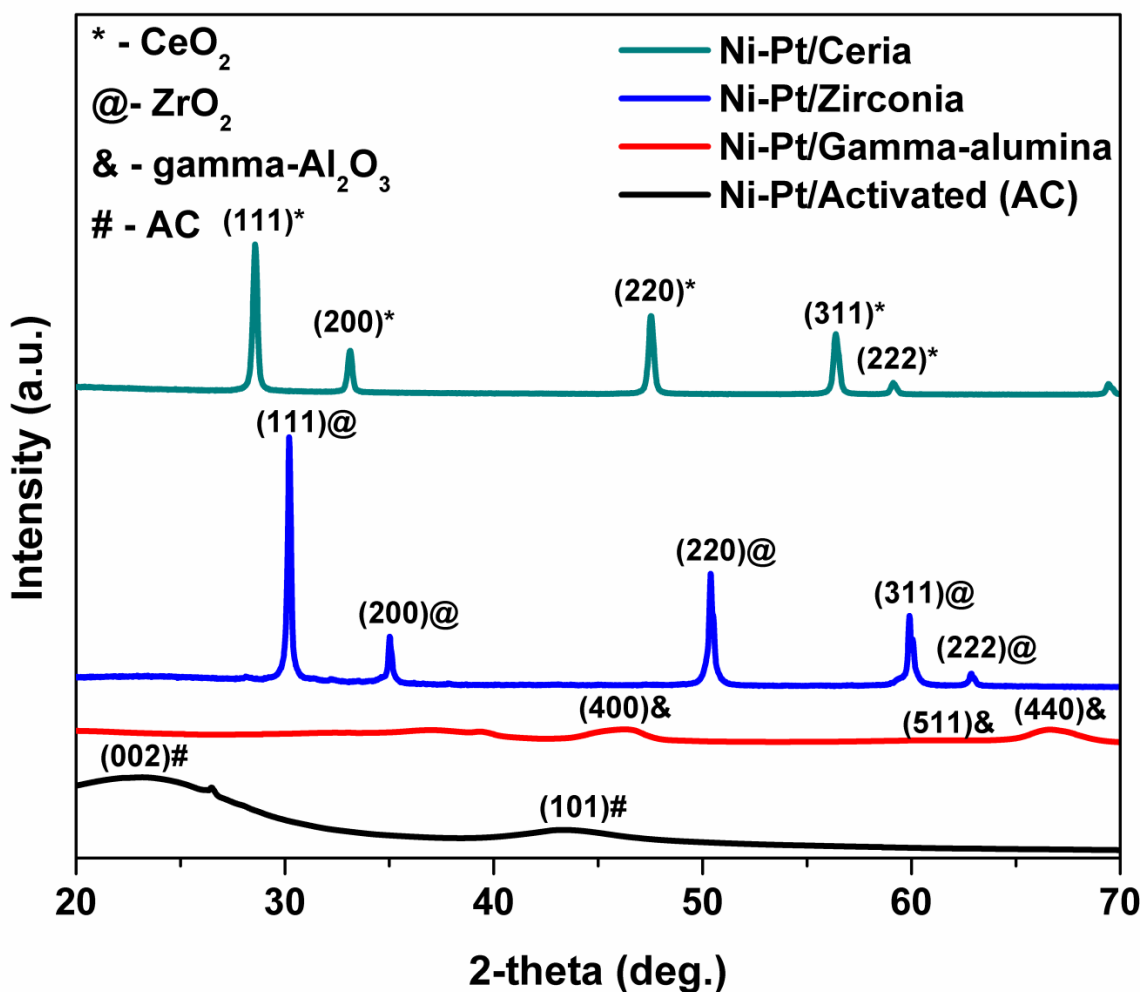


Figure 3. X-ray diffraction patterns of Ni(2.5%)-Pt(2.5%) catalysts loaded on different supports.

TEM micrographs of bimetallic Ni(2.5%)-Pt(2.5%) supported catalysts are shown in figure 4. The bimetallic Ni-Pt particles are homogeneously dispersed on support AC in the range of 4-8 nm (see figure 4a). Figure 4b revealed bimetallic Ni-Pt catalyst particles distributed on γ-alumina in the range of 5-8 nm. Figure 4c and 4d showed Ni-Pt particles supported on zirconia and ceria in

the ranges of 5-9 nm and 4-10 nm, respectively. The TEM micrographs showed spherical particles (encircled white).

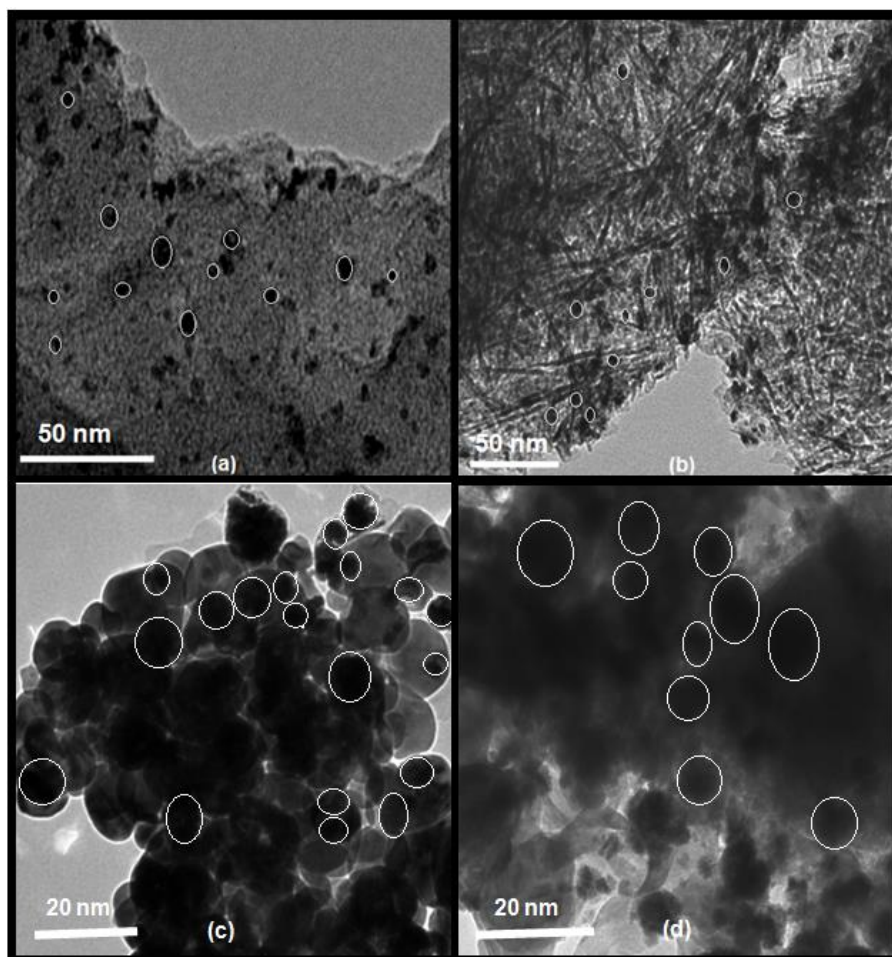


Figure 4. TEM micrographs of (a) Ni(2.5%)-Pt(2.5%)/AC, (b) Ni(2.5%)-Pt(2.5%)/ γ -alumina, (c) Ni(2.5%)-Pt(2.5%)/Zirconia, and (d) Ni(2.5%)-Pt(2.5%)/Cerium.

3.2. Catalytic performance and discussion

The effect of different supports (AC, γ -alumina, Zirconia, and Ceria) on hydrogen iodide conversion is presented in figure 5. Here, the thermodynamic-equilibrium conversions are also

shown at different temperatures in the range of 400°C-550°C. The conversion of hydrogen iodide increases on increasing the temperature, as this reaction is endothermic. Four different temperatures (400°C, 450°C, 500°C, and 550°C) were selected to test the catalysts performances. The catalytic performance for different supports alone followed the order: **AC > γ -alumina > Zirconia > Ceria**.

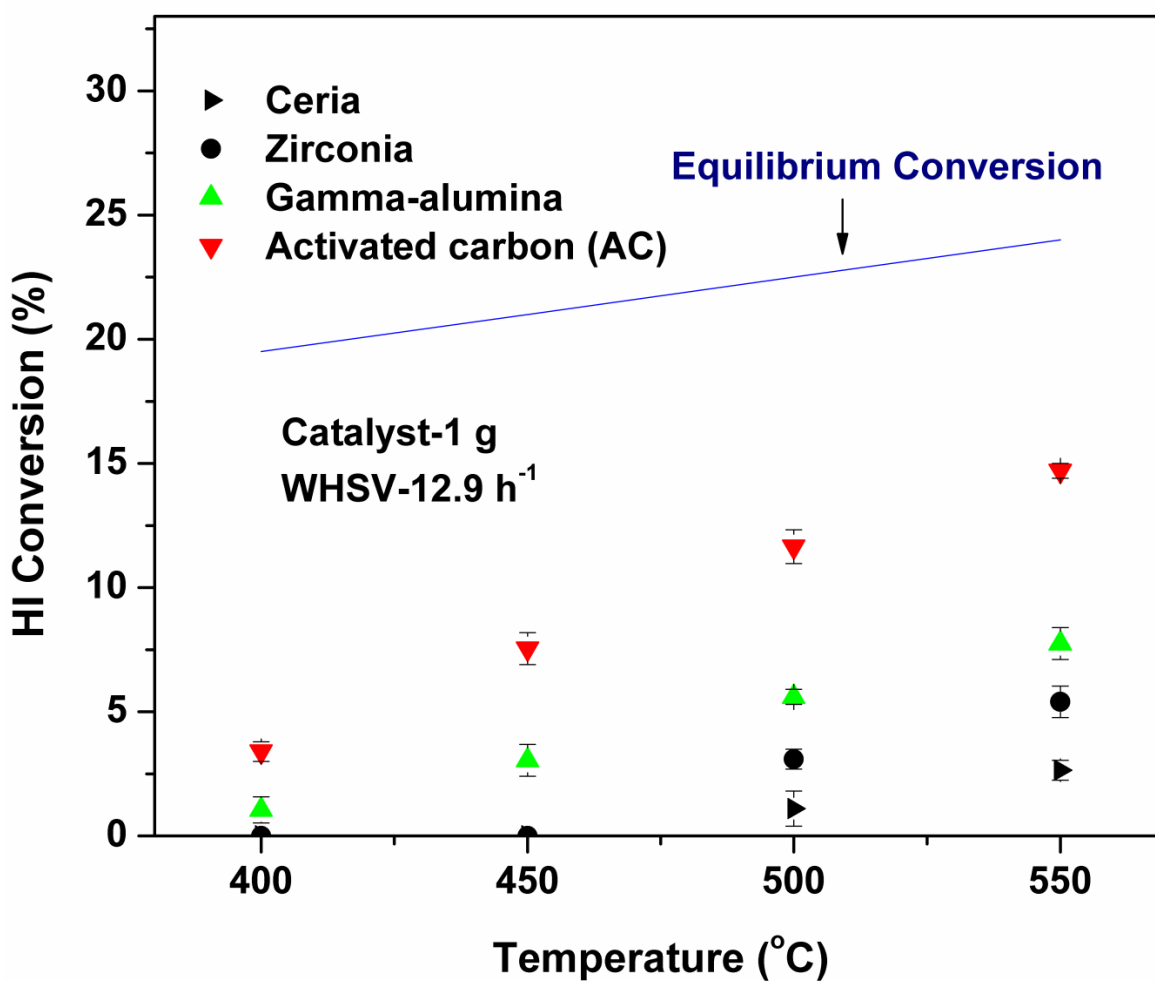


Figure 5. Catalytic activity of different supports (Cerium, Zirconia, γ -alumina, and AC), without the metallic loading, on hydrogen iodide conversion (HI-55 wt %).

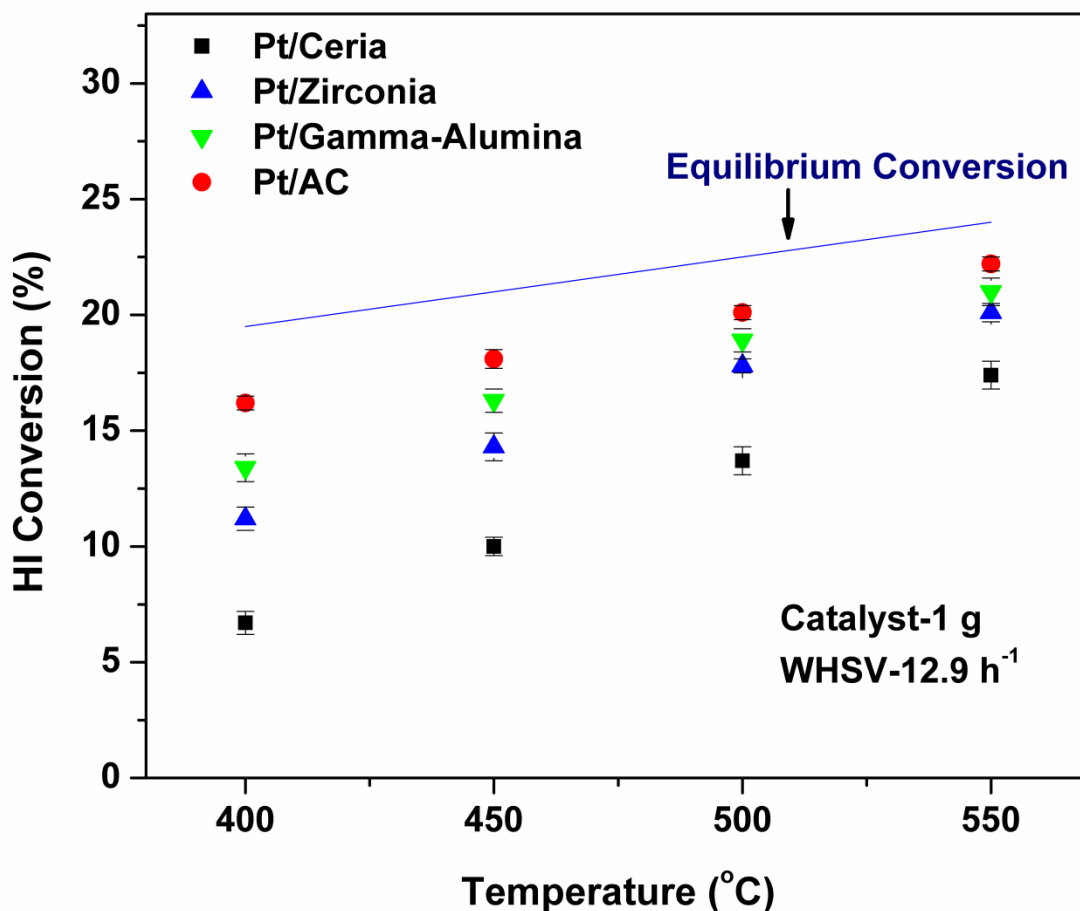


Figure 6. Activity of different supported Pt(2.5%) catalysts for hydrogen iodide-decomposition reaction (HI-55 wt%).

Figure 6 shows the activities of different supported monometallic Pt catalysts. Pt(2.5%)/AC showed the highest hydrogen iodide conversion among all the monometallic Pt catalysts. It showed conversions of 16.2% and 22.2% at 400°C and 550°C, respectively. Pt(2.5%)/Ceria showed the lowest hydrogen iodide conversions. The catalytic activities of different supported monometallic Pt followed the order: **Pt(2.5%)/AC > Pt(2.5%)/ γ -alumina > Pt(2.5%)/Zirconia > Pt(2.5%)/Ceria.**

The catalytic activities of bimetallic Ni-Pt catalysts deposited on different supports are shown in figure 7. The bimetallic Ni(2.5%)-Pt(2.5%)/Ceria showed a low hydrogen iodide conversion of 8.9% at 400°C, and this hydrogen iodide conversion was increased to 19.5% at 550°C. The Ni(2.5%)-Pt(2.5%)/Zirconia, Ni(2.5%)-Pt(2.5%)/ γ -alumina, and Ni(2.5%)-Pt(2.5%)/AC gave hydrogen iodide conversion of 13.4%, 16.2%, and 18.1% at 400°C. As expected, with increase in reaction temperature, the conversion also increased, giving hydrogen iodide conversion value of 22.1%, 23.4%, and 23.9% (very close to the theoretical equilibrium value of 24%) at 550°C. Due to the high dispersions of the Ni-Pt bimetallic phase, (particle sizes of ~ 10 nm or less), the catalytic activity is significant, even at 400°C, which is well within the stability of Hastelloy MoCs.

As seen clearly, Ni(2.5%)-Pt(2.5%)/AC exhibits a higher catalytic activity than the other three catalysts. This is likely due to the high surface area of Ni(2.5%)-Pt(2.5%)/AC catalyst. The catalytic activities of Ni-Pt catalysts on different supports followed the order: **Ni(2.5%)-Pt(2.5%)/AC > Ni(2.5%)-Pt(2.5%)/ γ -alumina > Ni(2.5%)-Pt(2.5%)/Zirconia > Ni(2.5%)-Pt(2.5%)/Ceria**, which may be correlated to the surface area of the support. As the temperature increases, the conversions for all catalyst-support combinations tend to merge after a certain temperature. Here, the equilibrium is approaching and the reaction rate approaches zero. The data also indicate that the reaction is kinetically controlled with the metallic dispersion playing a key role in determining the kinetics. The activity results of bimetallic (Ni-Pt) catalysts also showed that these have a higher catalytic activity as compared to the monometallic (Pt) catalysts. Possible synergistic interactions between metal and support will be investigated further in ongoing work, in a bid to understand clearly the role of the metal vis-à-vis the support.

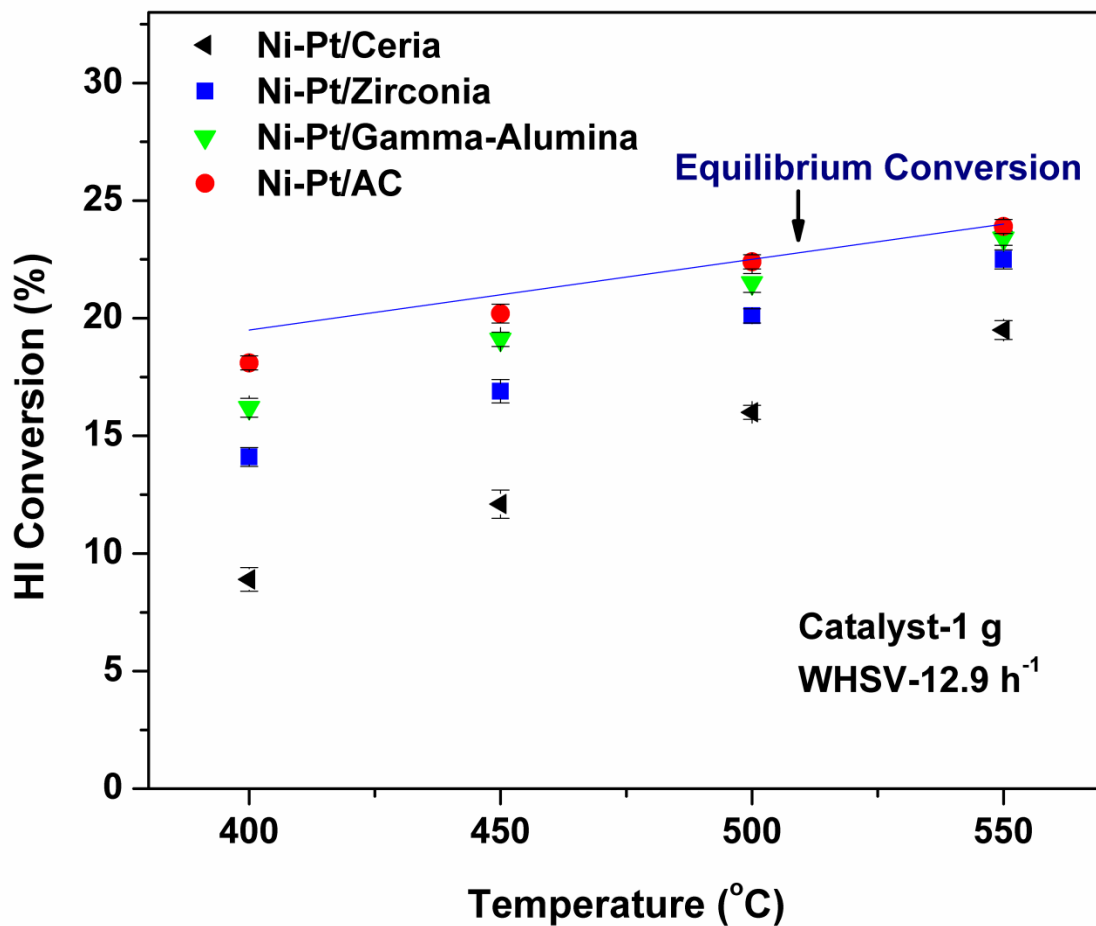


Figure 7. Activity of different supported Ni(2.5%)-Pt(2.5%) catalysts for hydrogen iodide-decomposition reaction (HI-55 wt%).

3.3. Stability of catalyst

The Ni(2.5%)-Pt(2.5%)/AC catalyst, which showed a very high dispersion, was run under steady state for 100 h. For this purpose, 2 g of the catalyst was put inside the reactor, and heated to 500°C. The Ni(2.5%)-Pt(2.5%)/AC exhibited a high catalytic activity, and an excellent stability up to a time period of 100 h. The measured HI conversion was constant (23.9%) for 100 h. No deactivation was observed during this time-period. Figure 8 shows time on stream (TOS) stability test of bimetallic Ni(2.5%)-Pt(2.5%)/AC for a time-period of 100 h.

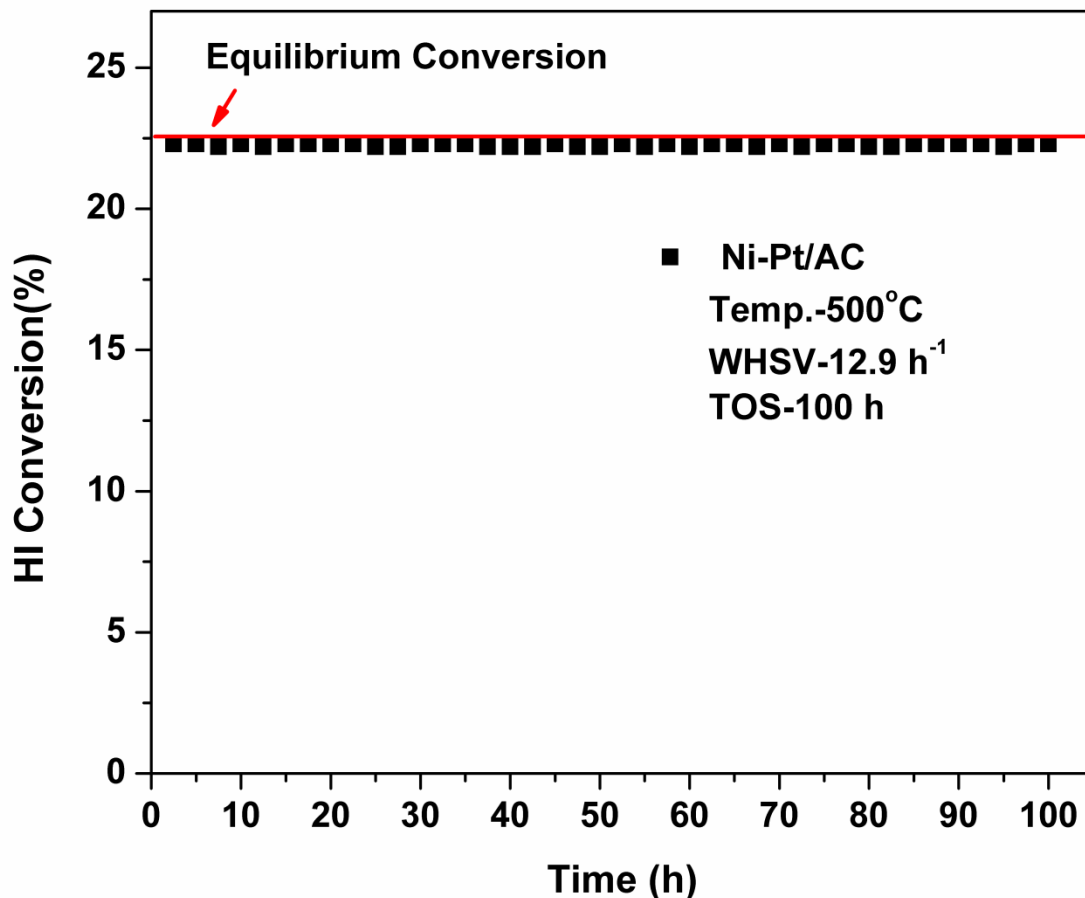


Figure 8. Time on stream (TOS) stability test of Ni(2.5%)-Pt(2.5%)/AC catalyst for hydrogen iodide conversion (Operating conditions: WHSV-12.9 h⁻¹, Temp.-500°C and TOS-100 h).

The average particle size of Ni-Pt particles in the spent-Ni(2.5%)-Pt(2.5%)/AC catalyst is about 5-11 nm (encircled white in figure 9) which indicates that the change of Ni-Pt particle size is not significant. From the TEM results, it could be deduced that the Ni-Pt bimetallic catalyst, demonstrates a high stability to sintering during hydrogen iodide decomposition, and appear to be resistant to corrosion, although advanced characterization experiments will be needed to observe the onset of corrosion over long times.

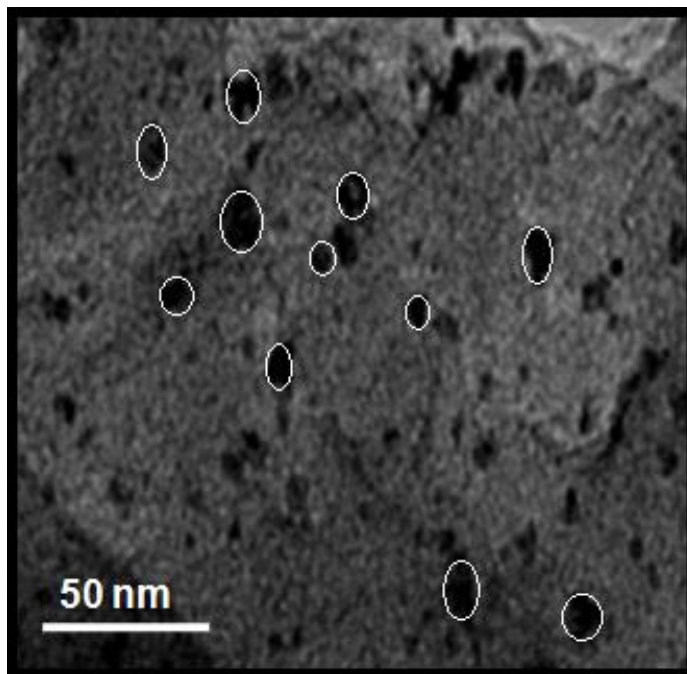


Figure 9. TEM micrograph of spent Ni(2.5%)-Pt(2.5%)/AC.

4. Conclusions

Bimetallic Ni(2.5%)-Pt(2.5%) catalyst nanoparticles supported on four different kinds of supports (AC, γ -alumina, Zirconia, and Ceria) were prepared successfully by a modified impregnation and chemical reduction technique. High levels of metallic dispersion were achieved with particle sizes being of the order of 10 nm or less, in the high surface area supports, and also verified by TEM micrographs. The catalytic activity of Ni-Pt catalyst on different supports showed the following order: Ni(2.5%)-Pt(2.5%)/AC > Ni(2.5%)-Pt(2.5%)/ γ -alumina > Ni(2.5%)-Pt(2.5%)/Zirconia > Ni(2.5%)-Pt(2.5%)/Ceria. Bimetallic Ni(2.5%)-Pt(2.5%)/AC catalyst showed the highest catalytic activity and excellent stability. The hydrogen iodide conversion of Ni(2.5%)-Pt(2.5%)/AC increased from 18.1 to 23.9%, over a temperature range 400°C to 550°C which is very close to the

equilibrium value. The catalyst performance was steady and stable for over 100 h, which appears to suggest that the particle size/ dispersions were sustainable at the reaction temperature. Therefore, bimetallic Ni(2.5%)-Pt(2.5%)/AC nanoparticles, synthesized by the method suggested, are a viable catalyst system which can operate at temperatures of 450°C as well, where MoCs like Hastelloy can be used. Further studies are in progress to explore higher Ni:Pt loadings, examining the synergistic effects of Ni-Pt bimetallic and the viability of transition metals like Ni, over a range of space velocities. A study of the kinetics and the hydrogen iodide-decomposition mechanism on transition metal catalyst is in progress, as well.

Acknowledgements

One of the authors (AS) wants to thank ONGC Energy Centre, India, for providing him with a Research Fellowship.

REFERENCES

- [1] Maeda K, Domen K. New non-oxide photocatalysts designed for overall water splitting under visible light. *J Phys Chem C* 2007;111:7851-61.
- [2] Winter CJ. Hydrogen energy-abundant, efficient, clean: a debate over the energy-system-of-change. *Int J Hydrogen Energy* 2009;34(14):S1-52.
- [3] Moriarty P, Honnery D. Hydrogen's role in an uncertain energy future. *Int J Hydrogen Energy* 2009;34(1):31-9.
- [4] Zhang Y, Wang Z, Zhou J, Cen K. Ceria as a catalyst for hydrogen iodide decomposition

- in sulfur-iodine cycle for hydrogen production. *Int J Hydrogen Energy* 2009;34(4):1688-95.
- [5] Roth M, Knoche KF. Thermochemical water splitting through direct HI-decomposition from H₂O/HI/I₂ solutions. *Int J Hydrogen Energy* 1989;14(8):545-9.
- [6] O'Keefe DR, Norman JH, Williamson DG. Catalysis research in thermochemical water-splitting processes. *Catal Rev* 1980;22(3):325-69.
- [7] Kubo S, Nakajima H, Kasahara S, Higashi S, Masaki T, Abe H, Onuki K. A demonstration study on a closed-cycle hydrogen production by the thermochemical water-splitting iodine-sulfur process. *Nucl Eng Des* 2004;233:347-54.
- [8] Oosawa Y, Kumagai T, Mizuta S, Kondo W, Takemori Y, Fujii K. Kinetics of the catalytic decomposition of hydrogen iodide in the magnesium–iodine thermochemical cycle. *Bull Chem Soc Jpn* 1981;54:742–8.
- [9] Goldstein S, Borgard JM, Vitart X. Upper bound and best estimate of the efficiency of the iodine sulphur-cycle. *Int J Hydrogen Energy* 2005;30(6):619-26.
- [10] Shindo Y, Ito N, Haraya K, Hakuta T, Yoshitome H. Kinetics of catalytic decomposition of hydrogen iodide in thermochemical hydrogen production. *Int J Hydrogen Energy* 1984;9(8):695-700.
- [11] Ito N, Shindo Y, Hakuta T, Yoshitome H. Enhanced catalytic decomposition of HI by using a microporous membrane. *Int J Hydrogen Energy* 1984;9(10):835-9.
- [12] Funk JE. Thermochemical hydrogen production: past and present. *Int J Hydrogen Energy* 2001;26(3):185-90.
- [13] Trester PW, Staley H. Gas Research Institute report, 80/00981, 1981.
- [14] Wong B, Buckingham RT, Brown LC, Russ BE, Besenbruch GE, Kaiparambil A, Santhanakrishnan R, Roy A. Construction materials development in sulfur-iodine

- thermochemical water-splitting process for hydrogen production. *Int J Hydrogen Energy* 2007;32(4):497-504.
- [15] Kasahara S, Kubo S, Hino R, Onuki K, Nomura M, Nakao SI. Flowsheet study of the thermochemical water-splitting iodine-sulfur process for effective hydrogen production. *Int J Hydrogen Energy* 2007;32(4):489-96.
- [16] Choi JY, Kim YS, Sah I, NO HC, Jang C. Corrosion resistances of alloys in high temperature hydrogen iodide gas environment for sulfur-iodine thermochemical cycle. *Int J Hydrogen Energy* 2014;39(27):14557-64.
- [17] Zhang Y, Wang Z, Zhou J, Liu J, Cen K. Effect of preparation method on platinum-ceria catalysts for hydrogen iodide decomposition in sulfur-iodine cycle. *Int J Hydrogen Energy* 2008;33(2):602-7.
- [18] Kim JM, Park JE, Kim YH, Kang KS, Kim CH, Park CS, Bae KK. Decomposition of hydrogen iodide on Pt/C-based catalysts for hydrogen production. *Int J Hydrogen Energy* 2008;33(19):4974-80.
- [19] Wang ZC, Wang LJ, Zhang P, Chen SZ, Xu JM, Chen J. Effect of preparation methods on Pt/alumina catalysts for the hydrogen iodide catalytic decomposition. *Chin Chem Lett* 2009;20(1):102-5.
- [20] Zhang Y, Zhou J, Chen Y, Wang Z, Liu J, Cen K. Hydrogen iodide decomposition over nickel-ceria catalysts for hydrogen production in the sulfur-iodine cycle. *Int J Hydrogen Energy* 2008;33(20):5477-83.
- [21] Favuzza P, Felici C, Lanchi M, Liberatore R, Mazzocchia CV, Spadoni A, Tarquini P, Tito AC. Decomposition of hydrogen iodide in the S-I thermochemical cycle over Ni catalyst systems. *Int J Hydrogen Energy* 2009;34(9):4049-56.

- [22] Chen Y, Wang Z, Zhang Y, Zhou Z, Cen K. Platinum-ceria-zirconia catalysts for hydrogen production in sulfur-iodine cycle. *Int J Hydrogen Energy* 2010;35(2):445-51.
- [23] Wang L, Hu S, Li D, Han Q, Zhang P, Chen S, Xu J. Effects of the second metals on the active carbon supported Pt catalysts for HI decomposition in the iodine-sulfur cycle. *Int J Hydrogen Energy* 2014;39(26):14161-65.
- [24] Wang Z, Wang L, Chen S, Zhang P, Xu J, Chen J. Decomposition of hydrogen iodide over Pt-Ir/C bimetallic catalyst. *Int J Hydrogen Energy* 2010;35(17):8862-67.
- [25] Li D, Wang L, Zhang P, Chen S, Xu J. Effects of the composition on the active carbon supported Pd-Pt bimetallic catalysts for HI decomposition in the iodine-sulfur cycle. *Int J Hydrogen Energy* 2013;38(16):6586-92.
- [26] Wang L, Bai S, Wang Z, Zhao Y, Yuan X, Zhang P, Chen S, Xu J, Meng X. Activity and stability of Pt catalysts supported on carbon nanotubes, active carbon and γ -Al₂O₃ for HI decomposition in iodine-sulfur thermochemical cycle. *Int J Hydrogen Energy* 2012;37(13):10020-7.
- [27] Wang L, Li D, Zhang P, Chen S, Xu J. The HI catalytic decomposition for the lab-scale H₂ producing apparatus of the iodine-sulfur thermochemical cycle. *Int J Hydrogen Energy* 2012;37(8):6415-21.
- [28] Wang L, Han Q, Li D, Wang Z, Chen J, Chen S, Zhang P, Liu B, Wen M, Xu J. Comparisons of Pt catalysts supported on active carbon, carbon molecular sieve, carbon nanotubes and graphite for HI decomposition at different temperatures. *Int J Hydrogen Energy* 2013;38(1):109-16.
- [29] Zhang Y, Wang Z, Zhou J, Liu J, Cen K. Catalytic decomposition of hydrogen iodide over pre-treated Ni/CeO₂ catalysts for hydrogen production in the sulfur-iodine cycle. *Int J*

- Hydrogen Energy 2009;34(21):8792-8.
- [30] Favuzza P, Felici C, Nardi L, Tarquini P, Tito A. Kinetics of hydrogen iodide decomposition over activated carbon catalysts in pellets. *Appl. Catal. B Environ.* 2011;105(1-2):30-40.
- [31] Wang L, Zhang P, Chen S, Xu J. Overview of the development of catalysts for HI decomposition in the iodine-sulfur thermochemical cycle at INET. *Nucl. Eng. Des.* 2014;271:60-63.
- [32] Bell AT. The impact of nanoscience on heterogenous catalysis. *Sci* 2003;299:1688-91.
- [33] Kim J, Lee Y, Sun S. Structurally ordered FePt nanoparticles and their enhanced catalysis for oxygen reduction reaction. *J Am Chem Soc* 2010;132:4996-7.
- [34] Wang R, Wang H, Wei B, Wang W, Lei Z. Carbon supported Pt-shell modified PdCo-core with electrocatalyst for methanol oxidation. *Int J Hydrogen Energy* 2010;35(19):10081-6.
- [35] Rachiero GP, Demirci UB, Miele P. Bimetallic RuCo and RuCu catalysts supported on γ -Al₂O₃. A comparative study of their activity in hydrolysis of ammonia-borane. *Int J Hydrogen Energy* 2011;36(12):7051-65.
- [36] Cheng F, Ma H, Li Y, Chen J. Ni_{1-x}Pt_x (x = 0-0.12) Hollow spheres as catalysts for hydrogen generation from ammonia borane. *Inorg Chem* 2007;46:788-94.
- [37] Yang X, Cheng F, Liang J, Tao Z, Chen J. Pt_xNi_{1-x} nanoparticles as catalysts for hydrogen generation from hydrolysis of ammonia borane. *Int J Hydrogen Energy* 2009;34(21):8785-91.
- [38] Shin WH, Jung HM, Choi YJ, Miyasaka K, Kang JK. Bimetallic catalysts selectively grown via N-doped carbon nanotubes for hydrogen generation. *J Mater Chem*

- 2010;20:6544-9.
- [39] Stamenkovic VR, Mun BS, Arenz M, Mayrhofer KJJ, Lucas CA, Wang G, Ross PN, Markovic NM. Trends in electrocatalysis on extended and nanoscale Pt-bimetallic alloy surfaces. *Nat Mater* 2007;6:241-7.
- [40] Zhao J, Sarkar A, Manthiram A. Synthesis and characterization of Pd-Ni nanoalloy electrocatalysts for oxygen reduction reaction in fuel cells. *Electrochim Acta* 2010;55(5):1756-65.
- [41] Greeley J, Stephens IE, Bondarenko AS, Johansson TP, Hansen HA, Jaramillo TF, Rossmeisi J, Chorkendorff I, Norskov JK. Alloys of platinum and early transition metals as oxygen reduction electrocatalysts. *Nat Chem* 2009;1:552-6.
- [42] Kolli NE, Delannoy L, Louis C. Bimetallic Au-Pd catalysts for selective hydrogenation of butadiene: Influence of the preparation method on catalytic properties. *J Catal* 2013;297:79-92.
- [43] Watson JM, Ozkan US. Spectroscopic characterization of surface species in deactivation of sol-gel Gd-Pd catalysts in NO reduction with CH₄ in the presence of SO₂. *J Catal* 2003;217(1):1-11.
- [44] Liu D, Quek XY, Cheo WNE, Lau R, Borgna A, Yang Y. MCM-41 supported nickel-based bimetallic catalysts with superior stability during carbon dioxide reforming of methane: Effect of strong metal-support interaction. *J Catal* 2009;266(2):380-90.
- [45] Rebelli J, Detwiler M, Ma S, Williams CT, Monnier JR. Synthesis and characterization of Au-Pd/SiO₂ bimetallic catalysts prepared by electroless deposition. *J Catal* 2010;270(2):224-33.
- [46] Aarikan T, Kannan AM, Kadirgan F. Binary Pt-Pd and ternary Pt-Pd-Ru

- nanoelectrocatalysts for direct methanol fuel cells. *Int J Hydrogen Energy* 2013;38:2090-7.
- [47] Zhou ZM, Shao ZG, Qin XP, Chen GX, Wei ZD, Yi BL. Durability study of Pt-Pd/C as PEMFC cathode catalyst. *Int J Hydrogen Energy* 2010;35:1719-26.
- [48] Hong P, Luo F, Liao S, Zeng J. Effects of Pt/C, Pd/C and PdPt/C anode catalysts on the performance and stability of airbreathing direct formic acid fuel cells. *Int J Hydrogen Energy* 2011;36:8518-24.
- [49] Wojcieszak R, Zieliński M, Monteverdi S, Bettahar MM. Study of nickel nanoparticles supported on activated carbon prepared by aqueous hydrazine reduction. *J Coll Interf Sci* 2006;299(1):238-48.
- [50] Chou KS, Chang SC, Huang KC. Study on the characteristics of nanosized nickel particles using sodium borohydride to promote conversion. *Adv Tech Mat Proc J (ATM, ISSN 1440-0731)* 2006;8:172-9.

List of Figures

Figure 1. Schematic diagram of preparation procedure of Ni-Pt catalyst loaded on different supports.

Figure 2. Schematic diagram of the experimental facility for testing of catalytic activity.

Figure 3. X-ray diffraction patterns of Ni-Pt catalysts loaded on different supports.

Figure 4. TEM micrographs of (a) Ni(2.5%)-Pt(2.5%)/AC, (b) Ni(2.5%)-Pt(2.5%)/ γ -alumina, (c) Ni(2.5%)-Pt(2.5%)/Zirconia, and (d) Ni(2.5%)-Pt(2.5%)/Cerium.

Figure 5. Catalytic activity of different supports (ceria, zirconia, γ -alumina, and AC), without the metallic loading, on hydrogen iodide conversion (HI-55 wt %).

Figure 6. Activity of different supported Pt(2.5%) catalysts for hydrogen iodide-decomposition reaction (HI-55 wt%).

Figure 7. Activity of different supported Ni(2.5%)-Pt(2.5%) catalysts for hydrogen iodide-decomposition reaction (HI-55 wt %).

Figure 8. Time on stream (TOS) stability test of Ni(2.5%)-Pt(2.5%)/AC catalyst for hydrogen iodide conversion (Operating conditions: WHSV-12.9 h⁻¹, Temp.-500°C and TOS-100 h).

Figure 9. TEM micrograph of spent Ni(2.5%)-Pt(2.5%)/AC.

List of Tables

Table 1. MoC candidates with their stand-up temperatures for hydrogen iodide reaction.

Table 2. BET sample characterization.